Aust. J. Phys., 1993, **46**, 3–13

The Challenge of the EMC Effect*

A. W. Thomas,[A] *K. Saito*[B] *and A. Michels*[C]

[A] Department of Physics and Mathematical Physics, University of Adelaide, P.O. Box 498, Adelaide, S.A. 5001, Australia.
[B] Physics Division, Tohoku College of Pharmacy, Sendai 981, Japan.
[C] Department of Theoretical Physics, Oxford University, 1 Keble Rd, Oxford, U.K.

Abstract

A number of relatively successful quark model descriptions of nuclear matter have recently been developed, based on a mean-field description of non-overlapping nucleons bound by the self-consistent exchange of σ and ω mesons. By combining one such model with a recently developed method of calculating structure functions for the free nucleon, we are able to make a microscopic calculation of the structure functions of finite nuclei (in the local density approximation). As well as providing a semi-quantitative understanding of existing data, the model suggests that the impulse approximation, used in many theoretical treatments of nucleon binding, may be quite unreliable.

1. Introduction

Since the discovery by the European Muon Collaboration (EMC) that the structure functions of nuclei do not all have the same shape (Aubert *et al.* 1983*a*, 1983*b*; Bodek *et al.* 1983; Arnold *et al.* 1984), there has been considerable further investigation. On the experimental side some features of the data, like the apparently dramatic increase in the sea with mass number, have become much less distinct. Other new features such as shadowing at small x have become apparent. However, the outstanding feature of the data, namely the softening of the valence quark distribution below $x = 0{\cdot}7$ (at which point Fermi motion takes over) has not changed much (Ashman *et al.* 1988; Benvenuti *et al.* 1987; Dasu *et al.* 1988).

While one would eventually like a unified theoretical treatment of all the features of the EMC data, in this work we shall be concerned only with the softening of the valence quark distribution, which is possibly its most surprising feature. Early attempts to understand this aspect of the data were based upon conventional ideas like nucleon binding, calculated in the impulse approximation (IA) (see e.g. Akulinichev *et al.* 1985; Akulinichev and Shlomo 1986; Dunne and Thomas 1986; Uchiyama and Saito 1988). Other ideas included a possible enhancement of the cloud of virtual pions around a nucleon in a nucleus (Llewellyn Smith 1983; Ericson and Thomas 1983; Berger *et al.* 1985). More exotic proposals included the possibility of multi-quark clusters (Krzywicki 1976; Pirner and Vary 1981; Saito and Uchiyama 1985) and quark percolation through the nucleus

* Paper presented at the Tenth AIP Congress, University of Melbourne, February 1992.

0004-9506/93/010003$05.00

(Nachtmann and Pirner 1984). Extensive work has also been put into the idea that the nucleon may swell in the nucleus (dynamical rescaling, Close *et al.* 1985). Here we extend to nuclei the same technique that has been successfully used to calculate free nucleon structure functions for the MIT bag model (Jaffe 1983; Signal and Thomas 1989; Schreiber *et al.* 1990, 1991).

In an earlier investigation (Thomas *et al.* 1989) we used the Guichon (1988) model in which nuclear matter consists of non-overlapping bags bound in the mean-field approximation (MFA) by the self-consistent exchange of scalar (σ) and vector (ω) mesons. Our results emphasised that the EMC effect provides information on the momentum *and* energy distribution of *quarks* in nuclei. In particular, the usual impulse approximation based on nuclear binding was shown to significantly overestimate the suppression of the nuclear valence quarks because of the neglect of the binding of the quarks that are spectators to the hard collision. This conclusion remains valid in the present work which is significantly more sophisticated. Moreover we shall see that it is possible to quantitatively understand the experimental data for finite nuclei in this treatment.

Because it is the energy *and* momentum distribution of quarks that matters, one needs a quark model for nuclear matter. At the present stage of development such models are necessarily quite crude. Here we use both the Guichon model *and* a further development along the lines of the Boguta (1981) model—which enables us to fit not only the binding energy and saturation density of nuclear matter, but also its surface energy and thickness.

In order to apply these models to finite nuclei we use the local density approximation

$$q_A^{(2)}(x,\mu^2) = \int d\boldsymbol{r}\rho(r) \int_x dy f(y,\rho) q_N^{(2)}\left(\frac{x}{y},\rho,\mu^2\right). \tag{1}$$

Here ρ is the nuclear density distribution, $f(y,\rho)$ accounts for Fermi motion and $q_N^{(2)}$ is the twist-2 quark distribution of the bound nucleon. Each of these components of the calculation will be described in the following sections, beginning with the nuclear models. Then we briefly review the calculation of twist-2 quark distributions for free nucleons, before explaining how it all comes together to give $q_A^{(2)}$ in the penultimate section. In the final section we present the results and discuss them together with some ideas for further work.

2. The Nuclear Model

Our admittedly simple model of nuclear matter is based upon the MIT bag model (Chodos *et al.* 1974) in its simplest form—without gluonic or pionic corrections. However, following Guichon (1988), we add a coupling between the quarks and isoscalar scalar (σ) and vector (ω) mesons. Neglecting nucleon overlap (except inasmuch as this is the true origin of these mesons) we regard each nucleon bag as the source of mean scalar and vector fields, $\bar{\sigma}$ and $\bar{\omega}$ respectively. In order to calculate the strength of this source, however, we solve the usual Dirac equation for the valence quark wave function including the coupling to these mesons. Clearly we have to carry out this solution self-consistently.

The model just described does give a reasonable value for the nuclear compressibility K, when the coupling constants g_σ and g_ω are adjusted to

reproduce the saturation energy and density of nuclear matter. We shall show some results using this model below. However, it is unsatisfactory for our purposes in several ways. Firstly, the well known problems of centre of mass (c.m.) motion are ignored in the model just described. Secondly, the large value of the mean vector field required is problematic (e.g. Yazaki 1990).

In order to deal with the first problem we self-consistently correct for the effect of spurious c.m. motion on the energy of the nucleon (bound or free) as suggested by Fleck *et al.* (1990). As they discovered, this alone reduces the value of $\bar{\omega}$ required. However, it can be reduced even further by (generalising Boguta 1981) adding some higher order terms to the scalar field part of the underlying Lagrangian, specifically terms in σ^3 and σ^4. The two extra parameters so introduced ($\bar{b}$ and $\bar{c}$ respectively) can be adjusted to reproduce the surface energy and thickness of nuclear matter. Within this model (which has independently been developed by Dey *et al.* 1991) the total energy per nucleon for nuclear matter is given by

$$E = \frac{\gamma}{(2\pi)^3\rho}\int d\boldsymbol{k}\sqrt{\boldsymbol{k}^2 + m_N^{*2}} + \frac{1}{2\rho}(m_\omega^2\bar{\omega}^2 + m_\sigma^2\bar{\sigma}^2) + \frac{1}{\rho}(\tfrac{1}{3}b\bar{\sigma}^3 + \tfrac{1}{4}c\bar{\sigma}^4)\,, \quad (2)$$

where $\gamma = 4$ (the degeneracy factor), ρ is the baryon density, m_ω and m_σ are the meson masses and $\bar{\omega}$ and $\bar{\sigma}$ are the ω and σ mean field values. The effective nucleon mass m_N^* includes the c.m. correction as in Fleck *et al.* (1990). Using the linear boundary condition for the nucleon bag in nuclear matter, its stationary condition ($dm_N^*/dR = 0$) and the self-consistency condition $dE/d\bar{\sigma} = 0$, we can obtain the eigenvalue of the lowest quark state, the strength of the σ field and the bag radius R in nuclear matter. The coupling constants, the compressibility and the effective nucleon mass in our model are listed in Table 1.

Table 1. Coupling constants, compressibility K and effective nucleon mass m_N^* at saturation density 0·15 fm^{-3}

The first row is for the Guichon (1988) model, the second is for the present full calculation. The coupling constants of the σ and ω mesons to nucleons, C_σ and C_ω, and the self-coupling constants for the σ meson are $\bar{b}$ and $\bar{c}$. Here C_σ, C_ω, K and m_N^* are quoted in MeV. The free bag radius R_0 is 0·6 fm and the free nucleon mass is fixed at 939 MeV

	C_σ	C_ω	$\bar{b}$	$\bar{c}$	K	m_N^*
Guichon	240·1	175·5	0·0	0·0	230	748
Full	53·0	3·0	0·8372	9·480	140	884

3. Calculating Nucleon Structure Functions

In recent years there have been a number of attempts to relate the quark models that have been so widely used in spectroscopic studies to data in the deep inelastic regime (Signal and Thomas 1989; Schreiber *et al.* 1990, 1991; Benesh and Miller 1989). It has been apparent for a long time that the sensible way to approach this is to use the models to calculate twist-2 parton distributions at some (a priori unknown) low momentum scale (μ^2) (Cabibbo and Petronzio 1977). At such a scale one knows that the valence quarks carry a sizeable fraction of the nucleon momentum. One can then evolve these distributions to higher values of Q^2, where the twist-2 piece dominates, using perturbative QCD.

A specific advantage of the approach developed at the University of Adelaide (see also a recent paper by Meyer and Mulders 1991) is that it guarantees the correct support for the calculated quark distributions.

Starting from the usual expression for the twist-2 quark distribution (Jaffe 1983):

$$q_N^{(2)}(x,\mu^2) = \frac{m_N}{2\pi}\int dx e^{-im_N xz}\langle N|\psi_+^\dagger(\zeta^-)\psi_+(0)|N\rangle_C\,, \tag{3}$$

where m_N is the mass of the nucleon, the field operator $\psi_+(0)$ is $(1+\alpha_3)\psi(0)/2$ and $\psi(0)$ destroys a quark at $\boldsymbol{r}=0$. The coordinate ζ^- is $(z;0,0,-z)$ so that the action of the two field operators is separated by a distance on the light-cone. In order to preserve the correct support for the quark distribution we insert a complete set of intermediate states between the field operators (Signal and Thomas 1989) and carry out the z-integral using translational invariance *before making any approximation.* For the nucleon itself and for the intermediate states we use translationally invariant Peierls–Yoccoz states. These will be two-quark (with mass in the region of $3/4\ m$) and three-quark one anti-quark (with mass of order $5/4\ m$) states. In the calculation of the anti-quark distribution $\bar{q}^{(2)}(x,\mu^2)$ (for which ψ and $\psi^\dagger$ are interchanged in equation 3) the dominant contribution is from a four-quark intermediate state (again with mass of order $5/4\ m$).

One novel feature of this calculation is that it is quite clear that the nucleon has an intrinsic sea—even in a model with just valence quarks, like the three-quark bag. Furthermore, as a result of the Pauli Exclusion Principle, this intrinsic sea will not be flavour symmetric (Signal and Thomas 1989). Indeed we will find more d–$\bar{d}$ pairs in the sea. (This is because with two spins and three colours one can insert d-quarks into five different 1s-states in a proton bag, whereas there are only four states available for u-quarks.) Clearly an asymmetry such as this will have important consequences for the Gottfried sum-rule (Signal *et al.* 1991; Melnitchouk *et al.* 1991).

The dominant piece of the valence quark distribution calculated from equation (3) is that involving a two-quark intermediate state. This term is controlled by two parameters, the bag radius and the mass. For the latter it is important to take into account the effect of gluon exchange, which raises the mass of a pair of quarks with spin 1 and lowers that of a spin 0 pair so that the resultant splitting is 200 MeV (Close and Thomas 1988). Rather than using the model for the contribution to the valence distribution from $3q$–$\bar{q}$ intermediate states, we simply use a phenomenological term of similar shape [say $(1-x)^7$] with a normalisation chosen to ensure that we have three valence quarks. Under QCD evolution, this phenomenological term moves to small x so that there is no significant uncertainty for $Q^2 < 5$ GeV^2 and $x < 0{\cdot}1$. It is also worth noting that at small x we are sensitive to long-distance physics [the important values of z in equation (3) are roughly up to order $(mx)^{-1}$] which is difficult to handle in any phenomenological quark model, so it will be difficult to do any better in the near future.

In Fig. 1 we show a comparison between the valence quark distribution of the proton calculated for a bag radius of $0{\cdot}8$ fm and various phenomenological fits which will be loosely referred to as 'data'. A priori we have no way to

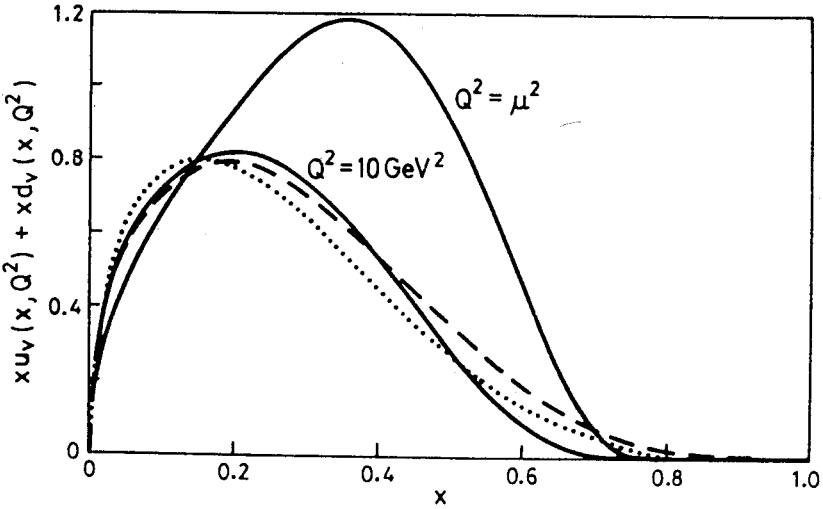

Fig. 1. The valence quark distribution, xF_3, calculated (Schreiber *et al.* 1990) for the bag model with a radius of 0·8 fm. The solid curves are calculated at the bag scale, μ^2, and evolved to 10 GeV^2. For comparison we show the fits to world data by Duke and Owens (1984) and Martin *et al.* (1988).

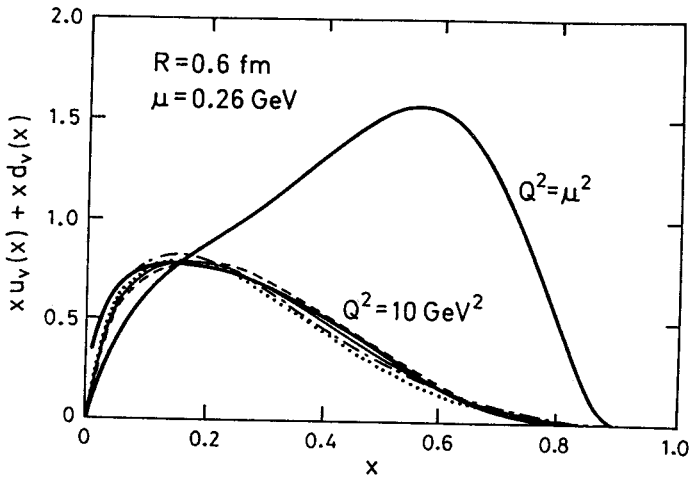

Fig. 2. Valence quark distributions, as in Fig. 1, but for $R = 0{\cdot}6$ fm. We also show the fits of Diemoz *et al.* (1988) and Eichten *et al.* (1986)—from Schreiber *et al.* (1991).

specify the bag scale μ. Instead it is determined by seeing how far one must evolve until the agreement with 'data' at 10 GeV^2 is optimal. Clearly the overall description of the 'data' is rather good. Only at very large values of x (>0·7) is there a significant difference. At such values the struck quark will have a momentum greater than 1 GeV/c and one would expect to have to include the

effect of correlations. There is an additional uncertainty associated with the use of leading order QCD, which may be less reliable for higher moments and hence large x.

On the other hand, the agreement with 'data' for calculations with a bag radius of 0·6 fm is essentially perfect (see Fig. 2). The improvement at large x is a consequence of the higher average momentum in the smaller cavity. Certainly it would be tempting to conclude that 0·6 fm is preferred. We choose not to draw that conclusion at this stage in view of the problems just cited. Instead we are content to observe that a bag with a radius in the range 0·6 to 0·8 fm gives a very good representation of the 'data'. Particularly for the calculations at 0·6 fm, the bag scale is rather low (e.g. 0·26 GeV in Fig. 2). For $\Lambda_{QCD} = 0{\cdot}2$ GeV, as used here, this gives a rather large value of $\alpha_s(\mu^2)$. Other phenomenological studies have used similar values in perturbative calculations of QCD evolution (Gluck *et al.* 1990), but we would be more comfortable with μ closer to 0·7 or 0·8 GeV. This does seem to be a likely, desirable consequence of including the pionic corrections needed to preserve chiral symmetry (Thomas 1991).

4. Nuclear Structure Functions

With both the quark-based nuclear model and a successful technique for calculating structure functions explained, we are ready to evaluate (1) to get the twist-2 nuclear structure function in the local density approximation (LDA). For the nuclear density distributions ρ_A, we use the phenomenological fits tabulated in Barrett and Jackson (1977). Fermi motion is treated through convolution of the quark distribution in the nucleon with the non-relativistic nucleon momentum distribution $f(y,\rho)$ appropriate to nuclear matter at density ρ (Llewellyn Smith 1983; Bickerstaff and Thomas 1989):

$$f(y,\rho) = \tfrac{3}{4}\left(\frac{m_N}{p_F}\right)^3 \left[\left(\frac{p_F}{m_N}\right)^2 - (y-1)^2\right]\theta\left(\frac{p_F}{m_N} - |y-1|\right), \tag{4}$$

$$\rho = \frac{\gamma}{6\pi^2} p_F^3 . \tag{5}$$

Finally, $q_N^{(2)}(x,\rho,\mu^2)$ is the twist-2 valence quark distribution of the nucleon bag, bound in nuclear matter of density ρ, and seen with resolution μ^2. The scale μ^2 is taken to be the same as that deduced by comparison with world data for a free nucleon of the same radius (when $\rho \to 0$) (Signal and Thomas 1989; Schreiber *et al.* 1990, 1991). In this way we omit any possible residual dynamical rescaling. In order to compare with actual nuclear data, the calculated distribution q_A is evolved (Schreiber *et al.* 1990), using leading order QCD, to $Q^2 = 10\ \mathrm{GeV}^2$. Finally, since it is usually F_2^A that is shown (rather than the valence distribution), we add a phenomenological sea quark distribution (Buras and Gaemers 1978) that (as apparently required by the data) is the same as in the free nucleon (apart from Fermi motion).

At the heart of the calculation is the twist-2 distribution $q_N^{(2)}(x,\rho,\mu^2)$. This is calculated at twelve values of the density between 0 and $1{\cdot}2\rho_0$ (nuclear matter density) and twenty values of x between zero and one. Standard spline

interpolation is then used to generate the value at arbitrary values of (x, ρ). Every step of this calculation has been tested independently and, as an overall check, two independent programs were written for the full calculation. For given parameters the final results are accurate to better than 1%.

Following the successful approach developed in Adelaide (Signal and Thomas 1989; Schreiber *et al.* 1990, 1991) for the free nucleon, we write the dominant piece of the twist-2 valence quark distribution for a bag, self-consistently bound in nuclear matter at density ρ, as

$$q_N^{(2)}(x,\rho,\mu^2) = \frac{m_N}{(2\pi)^3}\int d\boldsymbol{p}\,|\langle \widetilde{n{=}2,\boldsymbol{p}}|\psi_+(0)|\tilde{N}\rangle|^2\,\delta(\tilde{m}_N - m_N x - \tilde{p}^+_{n=2}), \qquad (6)$$

where $|\tilde{N}\rangle$ is the quark-level wave function of the bound nucleon, for which we use the Peierls–Yoccoz technique to construct a zero-momentum eigenstate. The field operator $\psi_+(0)$ is $(1+\alpha_3)\psi(0)/2$, where $\psi(0)$ destroys a quark at $\boldsymbol{r}=0$. Lastly, $|\widetilde{n{=}2,\boldsymbol{p}}\rangle$ is the wavefunction of the nucleon bag, in the medium, with one quark removed—again the Peierls–Yoccoz approximation is used to make a momentum eigenstate. Inside the delta-function, $\tilde{m}_N$ is the total energy of the bound nucleon, while $\tilde{p}^+_{n=2}$ is the plus component (p_0+p_z) of the 4-momentum of the bound *di-quark* bag. The inclusion of the binding of this residual pair is the crucial difference from the usual IA. Clearly it is easy to test the accuracy of the latter by replacing $|\widetilde{n{=}2,\boldsymbol{p}}\rangle$ and $\tilde{p}^+_{n=2}$ by the forms used in calculating the free nucleon structure function.

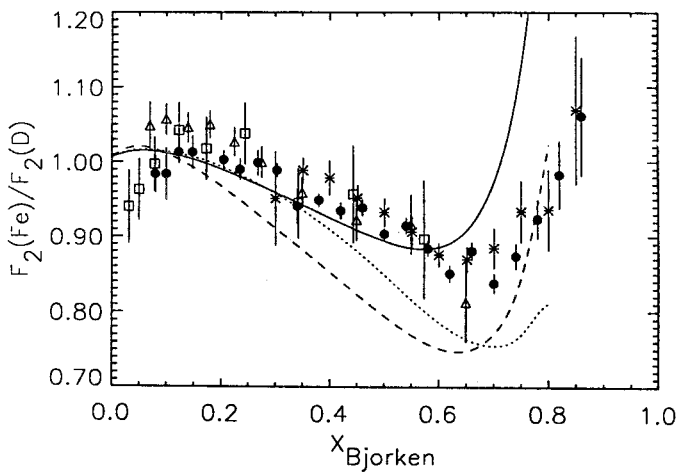

Fig. 3. EMC ratios (Fe/D) for the present full calculation (solid), the IA (dashed) and the Guichon model (dotted). The free bag radius is $R_0 = 0{\cdot}6$ fm and the cut-off momentum p_c is $1{\cdot}3$ fm^{-1}.

5. Results and Discussion

At last we are in a position to present the results. In Fig. 3 the solid curve is our complete calculation for the ratio of the structure functions of Fe and D (at 10 GeV^2), for the case where the free bag radius, R_0, is 0·6 fm. (The lack

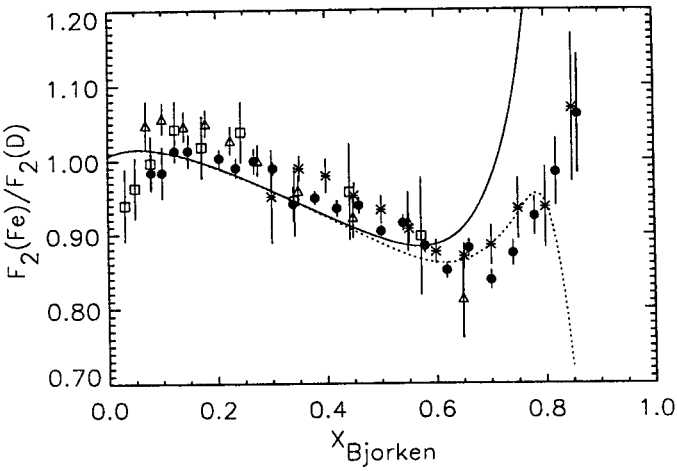

Fig. 4. Cut-off momentum dependence of Fe/D for $R_0 = 0{\cdot}6$ fm. The solid curve is for $p_c = 1{\cdot}3\ \mathrm{fm}^{-1}$, while the dotted curve involves no cut-off.

of sensitivity to R_0 is illustrated later.) For comparison we also show the most recent data from EMC, BCDMS and SLAC (Ashman *et al.* 1988; Dasu *et al.* 1988; Benvenuti *et al.* 1987). Clearly the calculation provides a semi-quantitative description of the data. Notice that one cannot use the local density approximation for deuterium. Instead we use a conventional convolution model allowing for 8 MeV binding and recoil (Bickerstaff and Thomas 1989; Dunne and Thomas 1986). The nucleon momentum distribution in D is given by the Paris potential (Lacombe *et al.* 1981). For the present our calculation of the nuclear structure functions includes no nucleon momenta higher than about $1{\cdot}3\ \mathrm{fm}^{-1}$. Therefore we have also imposed a cut-off (p_c) at $1{\cdot}3\ \mathrm{fm}^{-1}$ in the deuteron momentum wavefunction. That this only affects the EMC ratio at large x is shown in Fig. 4 where the dotted curve shows the ratio with no cut-off in the deuteron part of the calculation. The Guichon model which was discussed above predicts the ratio shown by the dotted curve in Fig. 3 which is not quite as good.

From the phenomenological point of view it is important to know whether our earlier conclusion about the inaccuracy of the IA remains true. The dashed curve in Fig. 3 shows the effect of ignoring the interaction of the residual two-quark bag with the nucleus. Clearly it dramatically overestimates the EMC effect. On physical grounds this makes good sense. Deep inelastic scattering measures the energy–momentum distribution of the struck *quark*, not the struck nucleon.

In Fig. 5 we illustrate the sensitivity of the results to the radius of the free bag—it is not strong. Finally, in Fig. 6, we show the prediction of the full model for the A-dependence of the EMC ratio. In general agreement with experiment, we find that as the atomic number increases the ratio is deeper for middle x and more enhanced for large x. However, as we have already remarked for Fe, the depth for large nuclei is not great enough.

Let us now briefly summarise our conclusions and comment on what remains to be done. It is very satisfying that a quark-level description of nuclear matter, together with the local density approximation and a microscopic method of

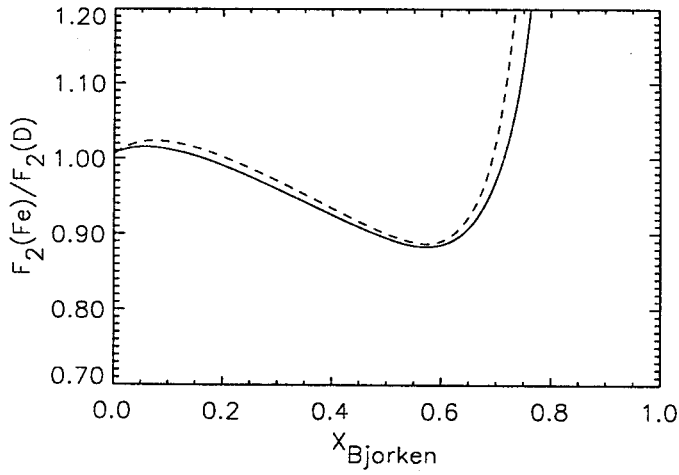

Fig. 5. Bag radius dependence of the ratio Fe/D for $p_c = 1{\cdot}3\ \mathrm{fm}^{-1}$. The solid and dashed curves are for $R_0 = 0{\cdot}6$ and $0{\cdot}8$ fm respectively.

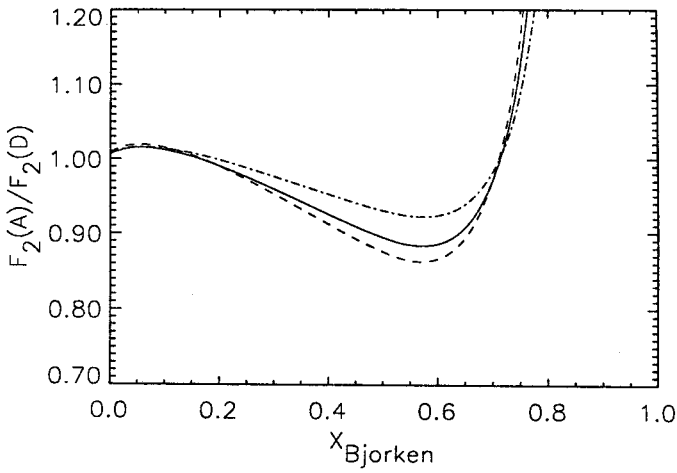

Fig. 6. Illustration of the dependence on atomic number with $R_0 = 0{\cdot}6$ fm and $p_c = 1{\cdot}3\ \mathrm{fm}^{-1}$. The dot-dashed, solid and dashed curves are for carbon, iron and gold respectively.

calculating twist-2 structure functions, does give a reasonable fit to the EMC data on Fe. Although it is disappointing in some ways that the impulse approximation fails, we have seen that there is a sound physical reason for this failure, namely that it effectively assigns the binding of an entire nucleon to a single struck quark. On the positive side we can be sure that nuclear deep inelastic scattering does tell us about the binding of quarks in nuclei.

Of course, having achieved this much one necessarily wants much more. One would like to go beyond the local density approximation, which would require a quark model for the structure of finite nuclei. It is also unsatisfactory to be

limited to a mean-field approximation for non-overlapping bags. Even though σ and ω exchange may be viewed, at least partly, as a macroscopic treatment of more complicated short-distance processes (perhaps involving quark and gluon exchange), one would like to do better.

The MIT bag model is also a fairly crude representation of nucleon structure. One should explore the consequences of using more sophisticated models—e.g. with a more reasonable surface, a better treatment of c.m. motion and perhaps a pion cloud. [The latter might eventually help us understand why there is no evidence for an enhancement in the pion field of the nucleus in recent Drell–Yan data (Garvey 1991).] As we have explained elsewhere (Schreiber *et al.* 1991; Thomas 1991), we are limited to leading order QCD unless the model used has a well defined connection to QCD.

Finally, our analysis has not yet had anything new to say about the nuclear sea or shadowing at small x. Eventually one may hope to understand all the features of the data within a single unified theory. That is the long-term challenge.

Acknowledgment

This work was supported by the Australian Research Council.

References

Akulinichev, S. V., and Shlomo, S. (1986). *Phys. Rev.* C **33**, 1551.
Akulinichev, S. V., Shlomo, S., Kulagin, S. A., and Vagradov, G. M. (1985). *Phys. Rev. Lett.* **55**, 2239.
Arnold, R. G., *et al.* (1984). *Phys. Rev. Lett.* **52**, 727.
Ashman, J., *et al.* (EMC Collaboration) (1988). *Phys. Lett.* B **202**, 603.
Aubert, J. J., *et al.* (EMC Collaboration) (1983*a*). *Phys. Lett.* B **123**, 275.
Aubert, J. J., *et al.* (1983*b*). *Nucl. Phys.* B **293**, 740.
Barrett, R., and Jackson, D. F. (1977). 'Nuclear Sizes and Structure' (Oxford Univ. Press).
Benesh, C. L., and Miller, G. A. (1989). *Phys. Lett.* B **222**, 476.
Benvenuti, A. C., *et al.* (BCDMS) (1987). *Phys. Lett.* B **189**, 483.
Berger, E. L., Coester, F., and Wiringa, R. B. (1985). *Phys. Rev.* D **29**, 398.
Bickerstaff, R. P., and Thomas, A. W. (1989). *J. Phys.* G **15**, 1523.
Bodek, A., *et al.* (SLAC) (1983). *Phys. Rev. Lett.* **50**, 1431.
Boguta, J. (1981). *Phys. Lett.* B **106**, 255.
Buras, A., and Gaemers, K. (1978). *Nucl. Phys.* B **132**, 249.
Cabibbo, N., and Petronzio, R. (1977). *Nucl. Phys.* B **126**, 298.
Chodos, A., Jaffe, R. L., Johnson, K., and Thorn, C. B. (1974). *Phys. Rev.* D **10**, 2599.
Close, F. E., Jaffe, R. L., Roberts, R. G., and Ross, G. G. (1985). *Phys. Rev.* D **31**, 1004.
Close, F. E., and Thomas, A. W. (1988). *Phys. Lett.* B **212**, 227.
Dasu, S., *et al.* (1988). *Phys. Rev. Lett.* **64**, 2591.
Dey, J., Tomio, L., Dey, M., and Frederico, T. (1991). *Phys. Rev.* C **44**, 2181.
Diemoz, M., *et al.* (1988). *Z. Phys.* C **39**, 21.
Duke, D. W., and Owens, J. T. (1984). *Phys. Rev.* D **30**, 49.
Dunne, G., and Thomas, A. W. (1986). *Nucl. Phys.* A **455**, 701.
Eichten, E., *et al.* (1986). *Rev. Mod. Phys.* **56**, 579.
Ericson, M., and Thomas, A. W. (1983). *Phys. Lett.* B **128**, 112.
Fleck, S., Bentz, W., Shimizu, K., and Yazaki, K. (1990). *Nucl. Phys.* A **510**, 731.
Garvey, G. T. (1991). *Nucl. Phys.* A **532**, 119c.
Gluck, M., Reya, E., and Vogelsang, W. (1990). *Nucl. Phys.* B **329**, 347.
Guichon, P. A. M. (1988). *Phys. Lett.* B **200**, 235.
Jaffe, R. L. (1983). *Nucl. Phys.* B **229**, 205.

Krzywicki, A. (1976). *Phys. Rev.* D **14**, 152.
Lacombe, M., *et al.* (1981). *Phys. Lett.* B **101**, 139.
Llewellyn Smith, C. H. (1983). *Phys. Lett.* **128** B, 107.
Martin, A., Roberts, R. G., and Stirling, W. J. (1988). *Phys. Rev.* D **37**, 1161.
Melnitchouk, M., Thomas, A. W., and Signal, A. I. (1991). *Z. Phys.* A **340**, 85.
Meyer, H., and Mulders, P. J. (1991). Nikhef preprint NIKHEF-P-12.
Nachtmann, O., and Pirner, H. J. (1984). *Z. Phys.* C **21**, 277.
Pirner, H. J., and Vary, J. P. (1981). *Phys. Rev. Lett.* **46**, 1376.
Saito, K., and Uchiyama, T. (1985). *Z. Phys.* A **322**, 299.
Schreiber, A. W., Thomas, A. W., and Londergan, J. T. (1990). *Phys. Rev.* D **42**, 2226.
Schreiber, A. W., Signal, A. I., and Thomas, A. W. (1991). *Phys. Rev.* D **44**, 2653.
Signal, A. I., and Thomas, A. W. (1989). *Phys. Rev.* D **40**, 2832.
Signal, A. I., Schreiber, A. W., and Thomas, A. W. (1991). *Mod. Phys. Lett.* A **6**, 271.
Thomas, A. W. (1991). *Nucl. Phys.* A **532**, 177.
Thomas, A. W., Michels, A., Schreiber, A. W., and Guichon, P. A. M. (1989). *Phys. Lett.* B **233**, 43.
Uchiyama, T., and Saito, K. (1988). *Phys. Rev.* C **38**, 2245.
Yazaki, K. (1990). *Prog. Nucl. Part. Phys.* **24**, 353.

Manuscript received 9 April, accepted 10 July 1992